Qualitative XANES and XPS Analysis of Substrate Effects in VO_2 Thin Films: A Route to Improving Chemical Vapour Deposition Synthetic Methods?

Michael J. Powell,[1] Ian J. Godfrey,[1] Raul Quesada-Cabrera,[1] Delphine Malarde,[1] Diana Teixeira,[1] Hermann Emerich,[2] Robert G. Palgrave,[1] Claire J. Carmalt,[1] Ivan P. Parkin,[1] Gopinathan Sankar[1]*

[1] Department of Chemistry, University College London, 20 Gordon Street, London. WC1H 0AJ, UK.

[2] Swiss-Norwegian Beamlines (BM01B), European Synchrotron Radiation Facilities, SNBL/ESRF, CS40220, 38043 Grenoble CEDEX 9, France.

*g.sankar@ucl.ac.uk

Abstract: Vanadium(IV) oxide thin films were synthesised *via* Atmospheric Pressure Chemical Vapour Deposition by the reaction between vanadium(IV) chloride and ethyl acetate at 550 °C. The substrate was varied with films being deposited on glass, SnO_2 and F-doped SnO_2. The films were characterised by X-ray diffraction, X-ray photoelectron spectroscopy, UV/vis spectroscopy, scanning electron microscopy and X-ray absorption near-edge structure. The influence of the electronic contribution of the substrate on the deposited VO_2 film was found to be key to the functional properties observed. Highly electron withdrawing substituents, such as fluorine, favoured the formation of V^{5+} ions in the crystal lattice and so reduced the thermochromic properties. By considering both the structural and electronic contributions of the substrate, it is possible to establish the best substrate choices for the desired functional properties of the VO_2 thin films synthesised.

1. Introduction:

Vanadium(IV) oxide materials have received widespread interest for functional applications in solar control coatings,[1-3] battery materials,[4, 5] gas sensing, data storage[6] and optical computing.[7, 8] The reason for such a wide range of functional properties is due in part to the variety of possible phases of VO_2 such as, monoclinic,[9] tetragonal,[10] VO_2(A)[11] and VO_2(B).[12] In these phases, small crystal lattice differences result in large measurable changes to the structural and electronic properties of the material.

For many of the above applications, thin films of VO_2 are desirable. Thin films of VO_2 have been successfully deposited *via* pulsed laser deposition,[13] RF sputtering,[14] metal organic chemical vapour deposition,[15] epitaxial growth,[16] aerosol assisted chemical vapour deposition (AACVD)[17] and atmospheric pressure chemical vapour deposition (APCVD).[18] Of these methods, APCVD has the desirable qualities of fast growth rates, conformal coatings and ease of delivery- *i.e*. there is no need for any vacuum systems or expensive reaction environments. APCVD, however, has limitations on the ability to form the differing polymorphs of VO_2.

One potential method to synthesise the various polymorphs of VO_2 is by growing on substrates which induce strain in the growing thin film- with the lattice mismatch promoting a particular phase due to a reduction in strain. This would allow for APCVD techniques to be expanded beyond the synthesis of monoclinic VO_2 thin films, to include phases such as VO_2(B) so that battery type structures could be deposited by this method. Another benefit of inducing strain in the surfaces would be improved crystallinity and properties of monoclinic VO_2 phases deposited. Additionally, the VO_2 metal-insulator transition comprises a change from the monoclinic to the rutile structure, during which substrate-induced electronic and structural effects are inherently involved;[19] consequently, control and understanding of these effects is a promising avenue of exploration for control over this transition.[20, 21]

To identify and characterise these effects, it is necessary to be able to probe the local structure, coordination environment and electronic structure of the V^{4+} ions. Since X-ray absorption near-edge structure (XANES) allows the determination of both the average oxidation state of and the average geometry surrounding a particular species. It is heavily influenced by electronic effects and is ideally suited to focus on the vanadium centres in VO_2.

In order to determine the effect of the substrate on the phase, local coordination environment and functional properties of film deposited by APCVD, we have combined X-ray diffraction, UV/vis spectroscopy, X-ray photoelectron spectroscopy, scanning electron microscopy and XANES to probe VO_2 thin films deposited on glass, SnO_2 and F-doped SnO_2 substrates. By combining these powerful techniques, it has been possible to determine how the substrate choice affects the formation of the vanadium(IV) oxide. Outlined in this paper is an in-depth study of the influence of the substrate on the local coordination environment of VO_2 thin films.

2. Experimental:

Vanadium(IV) chloride (99.9%), butyltin trichloride (95%), ammonium fluoride (98%), methanol (98%) and ethyl acetate (98%) were purchased from *Sigma Aldrich,* UK and used without further purification. The glass substrate used for depositions was 3.2 mm thick plain float glass with a 50 nm thick SiO_2 barrier layer (*Pilkington/NSG*). Depositions were carried out on Pilkington silica-coated barrier glass (50 nm SiO_2 coated on one side of float glass), with depositions occurring on the atmospheric (silica barrier) side of the glass in order to prevent unwanted leaching of ions from the glass into the thin film.[22] Prior to deposition, the glass substrates were cleaned with soapy water, isopropanol and acetone and were then left to air dry. The substrate was then loaded into the reaction chamber along with a second piece of float glass suspended 8 mm above (silica barrier layer pointing down) to ensure laminar flow during deposition.

2.1 Thin film synthesis

2.1.1 Deposition of SnO_2 and F-SnO_2 (FTO) substrates

SnO_2 and F-SnO_2 thin films were deposited on float glass *via* AACVD. A precursor solution was formed by dissolving butyltin trichloride (0.564 g: 0.002 mol) in 20 mL of methanol. In the case of F-SnO_2, ammonium fluoride (0.011 g: $3x10^{-4}$ mol) was added to the solution under rapid stirring conditions. An aerosol mist of the precursor solution was generated using a '*Liquifog*' piezo ultrasonic atomizer from *Johnson Matthey*, which uses an operating frequency of 1.6 MHz to produce a mode droplet size of *ca*. 3 µm. The mist was transported into the reactor through a baffle, using compressed air (21% (±0.5%) O_2 in N_2) supplied from *BOC* (UK) as the carrier gas, at a constant flow-rate of 1.0 L min^{-1}. The exhaust of the reactor was vented into a fume cupboard. The deposition was carried out at 550 °C. These films were subsequently used as substrates for the deposition of VO_2 thin films.

2.1.2 Deposition of VO_2 thin films

VO_2 thin films were synthesised using APCVD from reaction between vanadium(IV) chloride (VCl_4) and ethyl acetate (EtAc), following the procedure outlined by Malarde *et al*.[23] Briefly, the precursors were contained in stainless steel bubblers at appropriate temperature so as to generate enough vapour pressure through the system. For the synthesis of VO_2, the bubblers containing VCl_4 and EtAc were set to 80 and 40 °C, respectively, while the corresponding flow rates were set at 0.7 and 0.2 L min^{-1}, respectively. Nitrogen (oxygen free, 99 .9%, *BOC*) was used as the carrier gas. The gases were quickly mixed in stainless steel mixing chambers at 150 °C before entering the CVD reactor. A plain N_2 gas flow was set to 20 L min^{-1} in order to move the gas mixture into the reactor. The reactor was a 320 mm-long quartz tube containing a heating graphite block with three inserted Whatman heater cartridges. The reactor temperature was set to 550 °C. All lines in the system were heated to 200 °C using heating tape (*Electrothermal* 400 W, 230 V) and the temperature controlled using k-type thermocouples with *Thermotron* controllers.

In this work, the deposition times of the VO_2 films were varied between 30-180 s. For our discussion, VO_2 films of thicknesses of *ca*. 50 and 300 nm, deposited on barrier glass (thereafter, VO_2 *thin* and VO_2 *thick*, respectively), were used as reference samples. The discussion also includes VO_2 films of similar thicknesses (*ca*. 100 nm) deposited on SnO_2 and F-SnO_2 CVD films (thereafter, VO_2/TO and VO_2/FTO, respectively). These values were estimated from side-on scanning electron microscopy images. This information is summarised in Table 1 (*vide infra*).

2.2. Film characterisation

Scanning electron microscope (SEM) images were recorded on a *Jeol JSM-6301F* SEM instrument at an acceleration voltage of 5 kV. X-ray diffraction (XRD) patterns were recorded using a *Bruker D8 Discover* X-ray diffractometer using monochromatic Cu $K_{\alpha 1}$ and Cu $K_{\alpha 2}$ radiation of wavelengths 1.54056 and 1.54439 Å, respectively, emitted in an intensity ratio of 2:1 with a voltage of 40 kV and a current of 40 mA. The incident beam angle was 1° and data was collected between 5° and 66° (2θ) with a step size of 0.05° at 1.0 s/step. All diffraction patterns obtained were compared with database standards (ICSD). X-Ray photoelectron spectroscopy (XPS) was conducted on a *Thermo Scientific K-alpha* spectrometer with monochromated Al Kα radiation, a dual beam charge compensation system and constant pass energy of 50 eV (spot size 400 µm). Survey scans were collected in the binding energy range 0–1200 eV. High-resolution peaks were used for the principal peaks of V *2p*, Sn *3d*, O *1s* and C *1s*. Data was calibrated against C *1s* (binding energy, 285.0 eV). Data was fitted using *CasaXPS* software. Transmission spectra were recorded on a *Perkin Elmer Lambda 950* UV/vis/NIR spectrophotometer in transmission mode. A *Labsphere* reflectance standard was used as a reference for the UV/vis measurements.

V K-edge XANES measurements were carried out at BM01B, the Swiss-Norwegian beamlines at the European Synchrotron Radiation Facility (ESRF),[24] using a Si (111) double crystal monochromator detuned to 70% for harmonic rejection. Data were collected in fluorescence mode using a 13-element

Ge detector.[25] Data processing was carried out using Athena 0.9.25;[26] first, multiple scans from each film were merged to improve signal to noise ratio, then an edge-jump normalisation was performed.

3. Results and Discussion

3.1 Physical characterisation of VO_2 films

SEM analysis showed a marked difference in the morphology of the films by both the length of deposition and the substrate choice (Figure 1). When glass was used as the substrate, the initial deposition showed an island growth mechanism, with round crystallites present in the surface morphology (Figure 1a). With a deposition time of 3 mins, the crystallites exhibited large plate-like structures (Figure 1b), suggesting preferential orientation as the crystallites grow. The surface morphology was further altered when VO_2 was deposited on SnO_2 substrates. Figure 1c shows a VO_2 layer deposited onto the undoped SnO_2 substrate (sample VO_2/SnO_2), with large flat aggregated particles observed in the microstructure. In contrast, the VO_2 particles deposited on F-SnO_2 (sample VO_2/F-SnO_2) were smaller and the film consisted of several particle types including rod, plate and pyramidal like shapes. These morphologies are unquestionably influenced by the substrate, since the thicknesses of the VO_2 layers in both samples are identical, *i.e.* 100 nm (Table 1). It is worth noticing that typical SnO_2 and F-SnO_2 CVD films display different morphologies with rod- or pyramidal-like particles, respectively.[27, 28] Importantly, the difference in morphology could have an impact on the functional properties of the VO_2 films.[29]

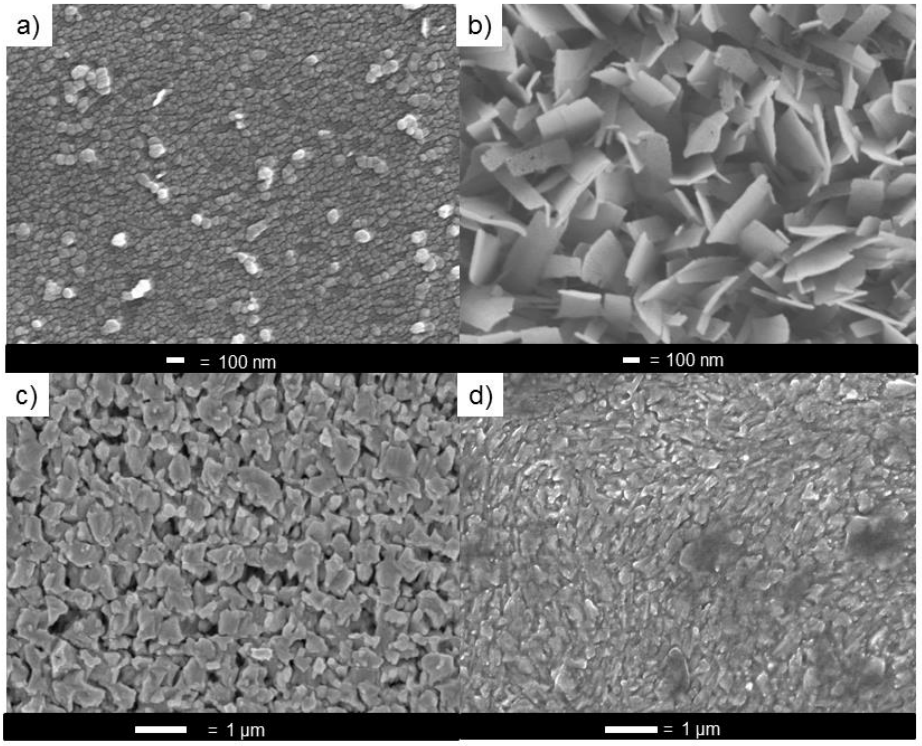

Figure 1: Typical SEM images of a) VO_2 *Thin*, b) VO_2 *Thick*, c) VO_2/TO and d) VO_2/FTO samples. All images show the surface morphology of VO_2 thin films deposited by APCVD on glass (a, b), SnO_2 (c) and F-SnO_2 (d) substrates.

XRD studies of the VO_2 films deposited on glass showed broad, weak diffraction peaks consistent with monoclinic VO_2 (Figure 2).[30] These patterns were similar to those obtained from typical VO_2 thin films deposited by CVD techniques.[31-33] No other phase of vanadium oxide was detected in these samples. The samples deposited on SnO_2–based substrates, however, could not be analysed by XRD due to overlap with the strong diffraction features of the substrate (Figure 2). These XRD patterns confirmed the presence of SnO_2 cassiterite structure ($P4_2$/mnm), with a tetragonal unit cell.[34] The XRD pattern of F-SnO_2 showed high relative intensities of diffraction peaks at 34.7 (200) and 52.4° (211), consistent with previous studies in the literature.[30, 31] Fluorine incorporation into SnO_2 has been previously shown to increase the intensity of these diffraction peaks.[35] This suggests that fluorine incorporation has been successful for the F-doped SnO_2 sample.

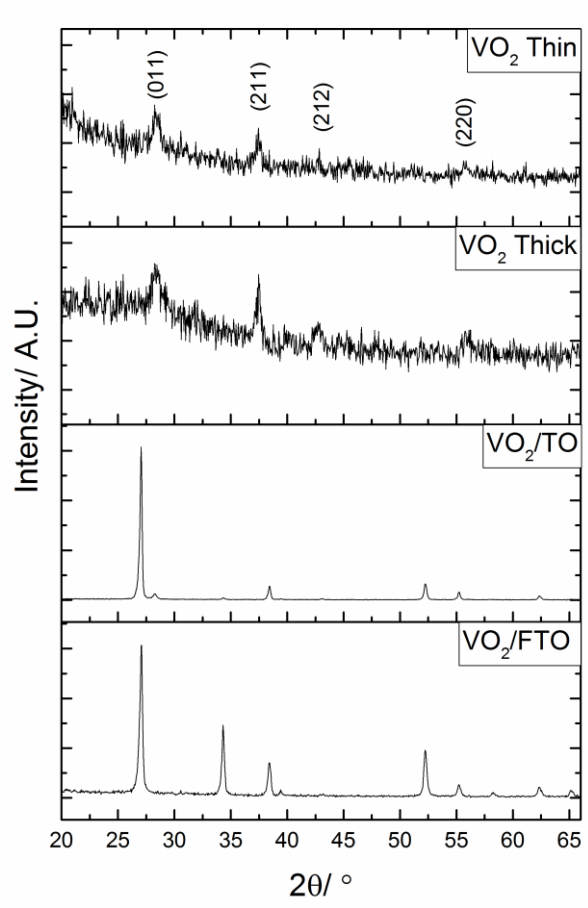

Figure 2: X-ray diffraction patterns of VO_2 films deposited on glass (VO_2 *thin* and VO_2 *thick*), SnO_2 (VO_2/TO) and F-SnO_2 (VO_2/FTO) substrates. The diffraction features observed in the former patterns confirmed the presence of monoclinic VO_2.

XANES and XPS results will now be discussed. Key to interpreting and rationalising these results is the difference in penetration depth of the techniques: XPS is surface sensitive, while XANES probes the bulk of the sample. As such, discrepancies between the results of these techniques provide information about the cross-section of the films. Additionally, the XPS will be substantially less influenced by substrate-film interactions.

The oxidation states of the elements present at the surface of the VO_2 thin films deposited on different substrates were probed by XPS analysis (Figure 3). In every spectrum, the V2$p_{3/2}$ environment could be resolved to give two binding energies at 517.1 and 515.7 eV, which are attributed to V^{5+} and V^{4+}, respectively, and within literature values (±0.2 eV).[36] Vanadium will readily oxidise in contact with air and fully-oxidised V^{5+} species are commonly found at the surface of vanadium oxide materials. Here,

the relative content of V^{5+} and V^{4+} species was similar across samples containing large VO_2 particles (Table 1), with a larger concentration of V^{5+} species. The opposite case, i.e. higher content of V^{4+} species, was however found in the case of sample VO_2 *thin*, deposited on glass. This can be attributed to the larger extent of surface area sampled along large particles, which is particularly clear along the plate-like structures in sample VO_2 *thick* (Figure 1b).

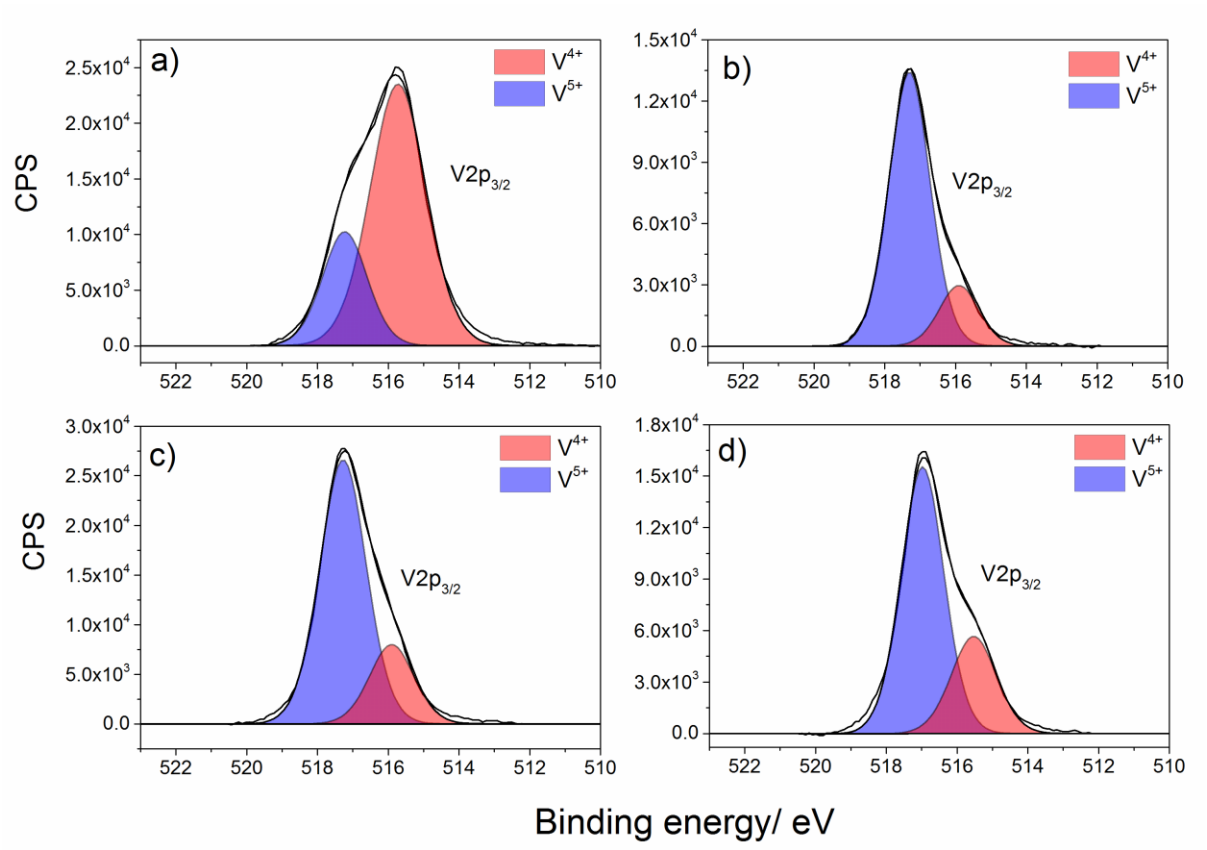

Figure 3: Typical XPS spectra in the $V2p_{3/2}$ environment for **a)** VO_2 *Thin*, **b)** VO_2 *Thick*, **c)** VO_2/TO and **d)** VO_2/FTO samples. CPS refers to *counts per second*.

Table 1: Description and properties of VO_2 films deposited onto different substrates by APCVD. Deposition times (s) and film thicknesses (nm) correspond to the VO_2 layers only. The latter were estimated by side-on SEM images. The relative content of different ionic species (%) were estimated from XPS analysis.

#	*Substrate*	*Dep. time*	*Thickness*	*Rel. content*

		(s)	*(nm)*	*(%)*	
				V^{5+}	V^{4+}
VO_2 *thin*	Glass	30	50	26	74
VO_2 *thick*	Glass	180	300	78	22
VO_2/TO	SnO_2	60	100	77	23
VO_2/FTO	F-SnO_2	60	100	65	35

Further insight into the different V^{n+} ionic species present in the VO_2 films was gained from XANES. Figure 4a shows XANES spectra of VO_2 thin films deposited on glass, SnO_2 and F-SnO_2 substrates, together with standard materials.

The pre-edge peak (*ca.* 5465 eV) provides insight into the speciation: the ratio of the pre-edge intensity to the edge jump is much, much greater in V_2O_5 than VO_2. From a visual inspection of the spectra, it is clear that this ratio indicates that VO_2, not V_2O_5, is the dominant component of the films. Despite the lack of structural assignment possible from the diffraction patterns of the SnO_2 supported forms, the distinctive pre-edge structure of V_2O_5 precludes it from being a majority component of the bulk of the film. This suggests, despite the XPS results, that all the samples are predominantly VO_2. Given that XPS is a surface sensitive technique, while XANES is a bulk technique, this discrepancy is hardly surprising – the XPS results will be influenced by the propensity of the exposed surface species to oxidise.

Figures 4b and 4c expand the edge region for the glass-supported and (F)TO supported films respectively. Interestingly, the edge position, for all the films, is closer to V_2O_5 than VO_2. This is probably the result of contributions from the surface V^{5+} species identified in the XPS and support-induced structural changes affecting electron energy levels.[36] Of particular relevance for the SnO_2 samples, structural changes arising from an RuO_2-covered substrate have previously been found to alter orbital occupancies.[37] This could conceivably affect the Fermi level, and RuO_2 has a similar

structure to the SnO_2 used herein (due to the remoteness of the surface from the interface, substrate-induced effects are not expected to influence the XPS measurements).

In the glass-supported films, VO_2 thick displays a pre-edge intensity (normalised μ(E) = 0.35) higher than that of VO_2 thin (normalised μ(E) = 0.24). These results are consistent with the XPS data, which shows VO_2 thick to contain more V^{5+} than VO_2 thin (78 % vs. 26 %, table 1).

This is, perhaps, a counter-intuitive observation – a thinner film would normally be expected to be the most susceptible to oxidation; or the surface to contribute more to the overall composition, at least – and suggests the possibility that the substrate has some kind of stabilising effect on the film. This can be corroborated by examination of the white-line (unoccupied p-states) and immediately post-edge regions: for VO_2 thin, these are substantially more intense than those for VO_2 thick (normalised μ(E) 1.31 vs 1.16 for the post-edge feature at 5489.5 eV) and the standards – indicating electron withdrawal. (To verify that this wasn't a consequence of increased self-absorption in the thicker film, the absorption length of VO_2 at 5515 eV was calculated, using Hephaestus[26] and XAFSMass,[38] and found to be *ca.* 6 μm – well above the thickness of these films (max *ca.* 300 nm).) This suggests that substrate-film electronic interactions may be present, as previously observed.[36] The relatively high strength of these interactions in VO_2 thin is easily explainable in terms of the proportion of atoms in the vicinity of the interface; for VO_2 thick, a greater proportion of the film is in the bulk, away from the interface, dampening this effect.

Electron withdrawal from the vanadium would also shift the edge to higher energy, as observed in figure 4b.

To summarise, in the region surrounding the film-substrate interface, the V^{4+} is stabilised against oxidation (possibly by electron transfer towards the substrate). This means that the thin film, of which a larger proportion is stabilised, experiences much less oxidation than the thicker one, which will have

greatest oxidation on the surface and greater oxidation than the thinner film in its bulk region as well as the stabilised interfacial region. This leads to the thicker film experiencing greater overall oxidation.

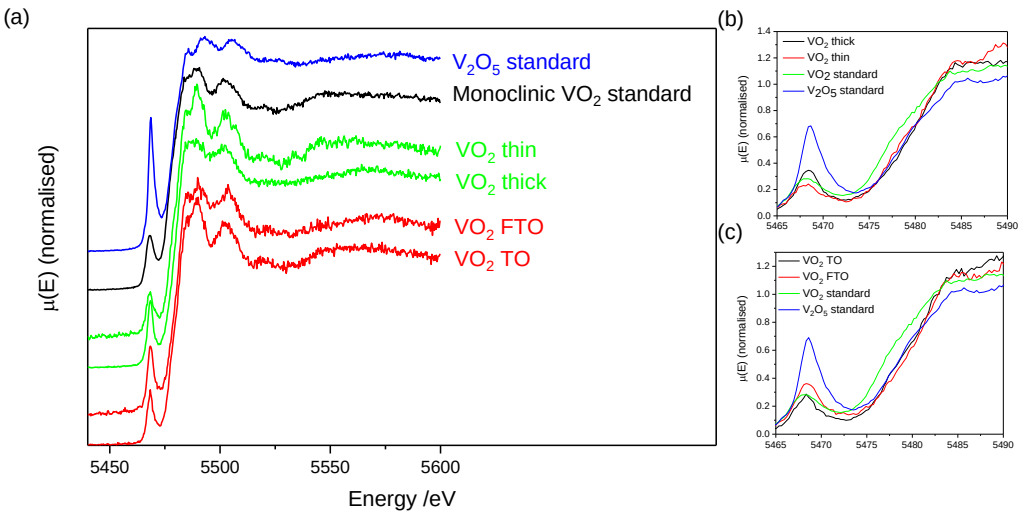

Figure 4: (a) Normalised XANES spectra for VO_2 thin films; (b) Expanded plot of edge region for films on glass; (c) Expanded plot of the edge region for films on TO/FTO

The relative intensities of the pre-edge peaks in the TO/FTO-supported samples are interesting: VO_2/F-SnO_2 displays a pre-edge intensity (normalised μ(E) = 0.36) higher than VO_2/SnO_2 (normalised μ(E) = 0.29), despite the XPS showing a slightly higher V^{5+} contribution in VO_2/SnO_2. Given the different penetration depths of the two techniques, this suggests that the oxidation-state ratio is not homogeneous throughout the film. Obviously, oxidation would be expected at the surface in both samples; however, in the F-doped film the vanadium species at the film-substrate interface will be in the vicinity of highly electronegative fluorine species. This could lead to substantial oxidation of the vanadium species in that region, accounting for the increased pre-edge intensity in the XANES.

Further evidence for the effect of fluorine is found by comparing the XPS with the XANES for the FTO-supported and thick, glass-supported films. These both show a similar V^{5+} contribution in the XANES pre-edge (normalised μ(E) = 0.36 and 0.35, respectively), however the FTO-supported film shows a reduced V^{5+} contribution in the XPS (65 % *vs.* 78%, respectively) – this indicates that, compared to the thick, glass-supported film, the V^{5+} in the FTO must be away from the surface. This difference in

distribution, strongly suggests that the additional V^{5+} in the FTO-supported film is likely to be near the substrate-film interface.

VO_2/SnO_2, VO_2/F-SnO_2 and the standards display the same basic post-edge structure: a small peak (V_2O_5) or shoulder (VO_2) at *ca.* 5484 eV followed by peaks at *ca.* 5490 eV and 5503 eV, followed by a broad minimum *ca.* 5517-5535 eV. The signal:noise ratio of the film spectra does not allow for a reliable distinction between peak and shoulder, however the feature at *ca.* 5484 eV is certainly more prominent in VO_2/SnO_2. The relative intensities of the two peaks in VO_2/SnO_2 are more consistent with the VO_2 standard (first peak more intense) than the V_2O_5 standard (both peaks equal). In VO_2/F-SnO_2, the difference in peak intensities is reduced, suggesting a greater V^{5+} contribution in this film – again consistent with increased oxidation.

In both cases, the intensity of the post-edge peaks is higher than in either of the standards, with the greatest increase shown by the VO_2/SnO_2. This is indicative of an increase in available *p*-states, which, as mentioned earlier, can have their occupancy reduced as a consequence of substrate-induced structural changes. Aetukuri *et al.* investigated this using an RuO_2 layer,[37] due to its structural similarity with metallic-phase rutile-VO_2; the SnO_2 used in this study also adopts a rutile structure, and so a similar effect may be causing the increased intensity. This could also explain why VO_2/SnO_2 displays a greater post-edge intensity boost than VO_2/F-SnO_2: FTO may distort from the "perfect" rutile structure and have a reduced level of effect on orbital occupancy. Electron transfer between the film and the substrate, as observed in the glass-supported films, could exist and could be responsible for this effect;[39] however, if that were the case, the more electronegative fluorine in the F-SnO_2 would be expected to display a more intense post-edge than the undoped SnO_2. This suggests that the structural effects dominate the electronic ones. The thin, gold-supported film displays the most intense post-edge – this is attributed to increased dominance of substrate-film interface effects in this film (half the thickness of the TO/FTO-supported films).

In keeping with this observation, the thicker film displays the distinctive green colour of V^{5+}, while the thinner film has a deeper brown hue, in keeping with typical colours for VO_2 thin films.

3.2 Thermochromic properties of VO_2 films

Variable temperature UV/vis spectra were obtained for all the samples prepared, Figure 5. As shown, all samples, except VO_2/F-SnO_2, displayed a thermochromic response when heated past the phase transition temperature. The thermochromic properties were fully reversible for samples VO_2 Thin, VO_2 Thick and VO_2/SnO_2 and were repeatable.

Sample VO_2/F-SnO_2 did not display any thermochromic behaviour. This supports the evidence found from the XANES analysis of this sample, where there was a high proportion of V^{5+}. With a high proportion of V^{5+} the sample would have insufficient VO_2 to convert between the monoclinic and tetragonal forms, and so would not be able to interact strongly with near IR wavelengths.

Although the sample on the F-doped SnO_2 substrate, VO_2/F-SnO_2, was not thermochromic, the visible light transmission in this sample was much higher than for any of the other samples analysed. This shows that the refractive properties of the substrate can affect the visible light transmission of the film. This is supports conclusions by Granqvist *et al*. who have shown that by reducing the change in refractive index, through the addition of multilayers, the visible light transmission of vanadium oxide thin films can be increased.[1, 40]

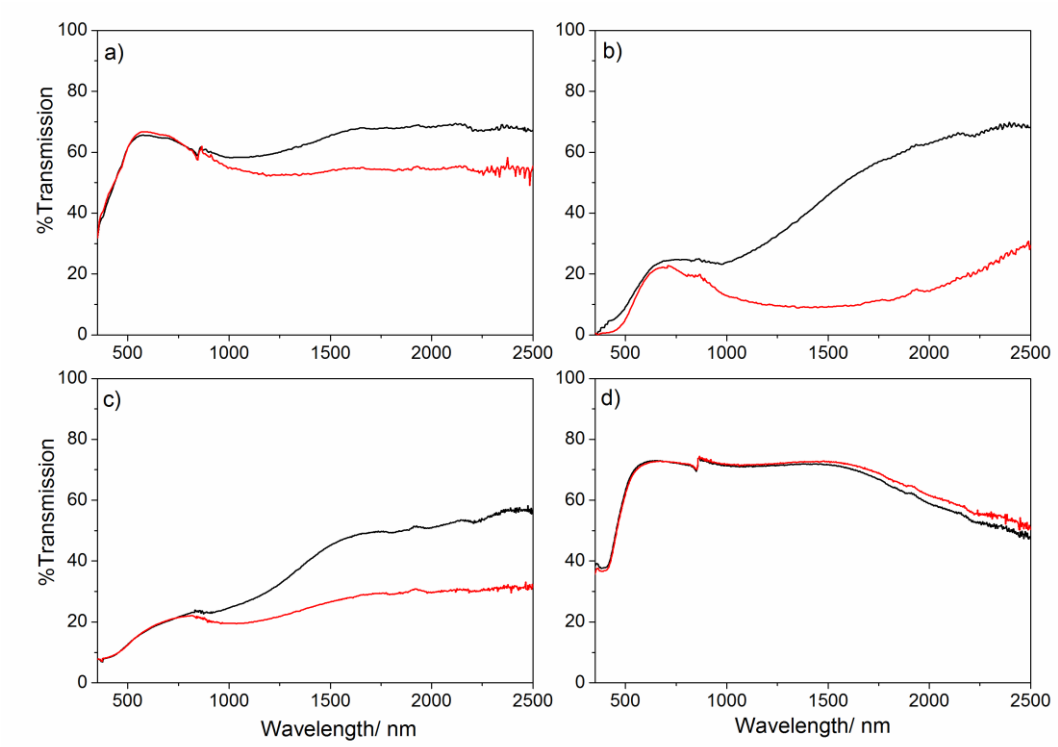

Figure 5: Typical variable temperature transmission UV/vis spectra for a) VO_2 Thin, b) VO_2 Thick, c) VO_2/SnO_2 and d) VO_2/F-SnO_2. Black lines represent %transmission at 25 °C and red lines %transmission at 80 °C. All VO_2 films were deposited at 550 °C by the reaction between vanadium(IV) chloride and ethyl acetate using atmospheric pressure chemical vapour deposition.

4. Conclusions

The choice of substrate can have a large impact on the properties of thin films of VO_2 deposited *via* APCVD techniques. By combining XANES, XPS and thermochromic measurements we have been able to successfully model why there is a marked difference in functional properties when depositing VO_2 onto various substrates. We have shown that when depositing onto crystalline substrates, the electronic contribution of the underlying substrate is key to understanding the properties observed. The electronic properties of the substrate, considering the band alignment and energetics of the substrate and VO_2, can lead to a destabilisation of V^{4+} ions and lead to an increase in V^{5+} and reduction in functional properties. Although it is possible to enhance the functional properties of monoclinic VO_2

by depositing onto substrates that will induce lattice matching, such as tetragonal SnO_2, the influence of substituents in the substrate must be carefully considered prior to depositions being conducted.

Acknowledgements

The authors would like to thank Drs Nuruzzaman Noor and Nicholas Chadwick for providing the SnO_2 and F-doped SnO_2 substrates for the study. MJP, CJC and IPP would like to thank the EPSRC for grant EP/L017709. IJG, RQC, IPP and GS would like to thank the EPSRC for grant EP/M003353/1. ESRF are thanked for beamtime on BM01B under proposal xxxx.

Author contributions

MJP and RQC synthesised VO_2 thin films for the study. MJP, RQC, DM, DT, HE and GS conducted synchrotron XANES measurements. IJG analysed and processed the XANES data. RGP, CJC, IPP and GS supervised the work. All authors contributed to the writing of the manuscript.

5. References

1. Granqvist, C. G.; Lansaker, P. C.; Mlyuka, N. R.; Niklasson, G. A.; Avendano, E., Progress in chromogenics: New results for electrochromic and thermochromic materials and devices. *Sol. Energy Mater. Sol. Cells* **2009,** 93, (Copyright (C) 2013 American Chemical Society (ACS). All Rights Reserved.), 2032-2039.
2. Parkin, I. P.; Binions, R.; Piccirillo, C.; Blackman, C. S.; Manning, T. D., Thermochromic coatings for intelligent architectural glazing. *Journal of Nano research* **2008,** 2, 1-20.
3. Warwick, M. E.; Binions, R., Advances in thermochromic vanadium dioxide films. *Journal of Materials Chemistry A* **2014,** 2, (10), 3275-3292.
4. Lübke, M.; Ding, N.; Powell, M. J.; Brett, D. J.; Shearing, P. R.; Liu, Z.; Darr, J. A., VO 2 nano-sheet negative electrodes for lithium-ion batteries. *Electrochemistry Communications* **2016,** 64, 56-60.
5. Niu, C.; Meng, J.; Han, C.; Zhao, K.; Yan, M.; Mai, L., VO2 nanowires assembled into hollow microspheres for high-rate and long-life lithium batteries. *Nano letters* **2014,** 14, (5), 2873-2878.
6. West, K. G.; Lu, J.; He, L.; Kirkwood, D.; Chen, W.; Adl, T. P.; Osofsky, M. S.; Qadri, S. B.; Hull, R.; Wolf, S. A., Ferromagnetism in Rutile Structure Cr Doped VO2 Thin Films Prepared by Reactive-Bias Target Ion Beam Deposition. *J. Supercond. Novel Magn.* **2008,** 21, (Copyright (C) 2013 American Chemical Society (ACS). All Rights Reserved.), 87-92.
7. Eden, D. D., Some applications involving the semiconductor-to-metal phase transition in vanadium dioxide. *Proc. Soc. Photo-Opt. Instrum. Eng.* **1979,** 185, (Copyright (C) 2013 American Chemical Society (ACS). All Rights Reserved.), 97-102.
8. Zhou, Y.; Chen, X.; Ko, C.; Yang, Z.; Mouli, C.; Ramanathan, S., Voltage-triggered ultrafast phase transition in vanadium dioxide switches. *IEEE Electron Device Lett.* **2013,** 34, (Copyright (C) 2013 American Chemical Society (ACS). All Rights Reserved.), 220-222.
9. Goodenough, J. B., Anomalous properties of the vanadium oxides. *Annu. Rev. Mater. Sci.* **1971,** 1, (Copyright (C) 2013 American Chemical Society (ACS). All Rights Reserved.), 101-38.
10. Goodenough, J. B., Two components of the crystallographic transition in vanadium dioxide. *Journal of Solid State Chemistry* **1971,** 3, (Copyright (C) 2013 American Chemical Society (ACS). All Rights Reserved.), 490-500.
11. Oka, Y.; Ohtani, T.; Yamamoto, N.; Takada, T., Phase transition and electrical properties of VO2 (A). *Nippon seramikkusu kyokai gakujutsu ronbunshi* **1989,** 97, (10), 1134-1137.
12. Mai, L.; Wei, Q.; An, Q.; Tian, X.; Zhao, Y.; Xu, X.; Xu, L.; Chang, L.; Zhang, Q., Nanoscroll Buffered Hybrid Nanostructural VO2 (B) Cathodes for High-Rate and Long-Life Lithium Storage. *Advanced Materials* **2013,** 25, (21), 2969-2973.
13. Kim, D.; Kwok, H. S., Pulsed laser deposition of VO2 thin films. *Applied physics letters* **1994,** 65, (25), 3188-3190.
14. Kana, J. K.; Ndjaka, J.; Ateba, P. O.; Ngom, B.; Manyala, N.; Nemraoui, O.; Beye, A.; Maaza, M., Thermochromic VO 2 thin films synthesized by rf-inverted cylindrical magnetron sputtering. *Applied Surface Science* **2008,** 254, (13), 3959-3963.
15. Sahana, M.; Dharmaprakash, M.; Shivashankar, S., Microstructure and properties of VO 2 thin films deposited by MOCVD from vanadyl acetylacetonate. *Journal of Materials Chemistry* **2002,** 12, (2), 333-338.
16. Kim, H.; Charipar, N.; Osofsky, M.; Qadri, S.; Piqué, A., Optimization of the semiconductor-metal transition in VO2 epitaxial thin films as a function of oxygen growth pressure. *Applied physics letters* **2014,** 104, (8), 081913.
17. Piccirillo, C.; Binions, R.; Parkin, I. P., Nb-doped VO2 thin films prepared by aerosol-assisted chemical vapour deposition. *Eur. J. Inorg. Chem.* **2007**, (Copyright (C) 2013 American Chemical Society (ACS). All Rights Reserved.), 4050-4055.
18. Powell, M. J.; Quesada-Cabrera, R.; Taylor, A.; Teixeira, D.; Papakonstantinou, I.; Palgrave, R. G.; Sankar, G.; Parkin, I. P., Intelligent Multifunctional VO2/SiO2/TiO2 Coatings for Self-Cleaning, Energy-Saving Window Panels. *Chemistry of Materials* **2016,** 28, (5), 1369-1376.

19. Liu, M.; Wagner, M.; Zhang, J.; McLeod, A.; Kittiwatanakul, S.; Fei, Z.; Abreu, E.; Goldflam, M.; Sternbach, A. J.; Dai, S., Symmetry breaking and geometric confinement in VO2: Results from a three-dimensional infrared nano-imaging. *Applied physics letters* **2014,** 104, (12), 121905.
20. Cui, Y.; Ramanathan, S., Substrate effects on metal-insulator transition characteristics of rf-sputtered epitaxial VO2 thin films. *Journal of Vacuum Science & Technology A: Vacuum, Surfaces, and Films* **2011,** 29, (4), 041502.
21. Muraoka, Y.; Hiroi, Z., Metal-insulator transition of VO2 thin films grown on TiO2 (001) and (110) substrates. *Applied physics letters* **2002,** 80, (4), 583-585.
22. Kafizas, A.; Crick, C.; Parkin, I. P., The combinatorial atmospheric pressure chemical vapour deposition (cAPCVD) of a gradating substitutional/interstitial N-doped anatase TiO2 thin-film; UVA and visible light photocatalytic activities. *Journal of Photochemistry and Photobiology a-Chemistry* **2010,** 216, (2-3), 156-166.
23. Malarde, D.; Powell, M. J.; Quesada-Cabrera, R.; Wilson, R. L.; Carmalt, C. J.; Sankar, G.; Parkin, I. P.; Palgrave, R. G., Optimized Atmospheric-Pressure Chemical Vapor Deposition Thermochromic VO2 Thin Films for Intelligent Window Applications. *ACS Omega* **2017,** 2, (3), 1040-1046.
24. van Beek, W.; Safonova, O. V.; Wiker, G.; Emerich, H., SNBL, a dedicated beamline for combined in situ X-ray diffraction, X-ray absorption and Raman scattering experiments. *Phase Transitions* **2011,** 84, (8), 726-732.
25. Abdala, P. M.; Safonova, O. V.; Wiker, G.; van Beek, W.; Emerich, H.; van Bokhoven, J. A.; Sá, J.; Szlachetko, J.; Nachtegaal, M., Scientific opportunities for heterogeneous catalysis research at the SuperXAS and SNBL beam lines. *CHIMIA International Journal for Chemistry* **2012,** 66, (9), 699-705.
26. Ravel, B.; Newville, M., ATHENA, ARTEMIS, HEPHAESTUS: data analysis for X-ray absorption spectroscopy using IFEFFIT. *Journal of synchrotron radiation* **2005,** 12, (4), 537-541.
27. Mathur, S.; Sivakov, V.; Shen, H.; Barth, S.; Cavelius, C.; Nilsson, A.; Kuhn, P., Nanostructured films of iron, tin and titanium oxides by chemical vapor deposition. *Thin Solid Films* **2006,** 502, (1), 88-93.
28. Sheel, D.; Yates, H.; Evans, P.; Dagkaldiran, U.; Gordijn, A.; Finger, F.; Remes, Z.; Vanecek, M., Atmospheric pressure chemical vapour deposition of F doped SnO 2 for optimum performance solar cells. *Thin Solid Films* **2009,** 517, (10), 3061-3065.
29. Vernardou, D.; Pemble, M. E.; Sheel, D. W., The Growth of Thermochromic VO2 Films on Glass by Atmospheric-Pressure CVD: A Comparative Study of Precursors, CVD Methodology, and Substrates. *Chemical Vapor Deposition* **2006,** 12, (5), 263-274.
30. Rogers, K., An X-ray diffraction study of semiconductor and metallic vanadium dioxide. *Powder Diffraction* **1993,** 8, (04), 240-244.
31. Manning, T. D.; Parkin, I. P., Atmospheric pressure chemical vapour deposition of tungsten doped vanadium(iv) oxide from VOCl3, water and WCl6. *J. Mater. Chem.* **2004,** 14, (Copyright (C) 2013 American Chemical Society (ACS). All Rights Reserved.), 2554-2559.
32. Manning, T. D.; Parkin, I. P.; Clark, R. J. H.; Sheel, D.; Pemble, M. E.; Vernadou, D., Intelligent window coatings: atmospheric pressure chemical vapour deposition of vanadium oxides. *J. Mater. Chem.* **2002,** 12, (Copyright (C) 2013 American Chemical Society (ACS). All Rights Reserved.), 2936-2939.
33. Pan, M.; Zhong, H.; Wang, S.; Liu, J.; Li, Z.; Chen, X.; Lu, W., Properties of VO2 thin film prepared with precursor VO(acac)2. *J. Cryst. Growth* **2004,** 265, (Copyright (C) 2013 American Chemical Society (ACS). All Rights Reserved.), 121-126.
34. Chang, E.; Graham, E., The elastic constants of cassiterite SnO2 and their pressure and temperature dependence. *Journal of Geophysical Research* **1975,** 80, (17), 2595-2599.
35. Acosta, D.; Zironi, E.; Montoya, E.; Estrada, W., About the structural, optical and electrical properties of SnO2 films produced by spray pyrolysis from solutions with low and high contents of fluorine. *Thin Solid Films* **1996,** 288, (1-2), 1-7.

36. Silversmit, G.; Depla, D.; Poelman, H.; Marin, G. B.; De Gryse, R., Determination of the V2p XPS binding energies for different vanadium oxidation states (V 5+ to V 0+). *Journal of Electron Spectroscopy and Related Phenomena* **2004,** 135, (2), 167-175.
37. Aetukuri, N. B.; Gray, A. X.; Drouard, M.; Cossale, M.; Gao, L.; Reid, A. H.; Kukreja, R.; Ohldag, H.; Jenkins, C. A.; Arenholz, E., Control of the metal-insulator transition in vanadium dioxide by modifying orbital occupancy. *Nature Physics* **2013,** 9, (10), 661-666.
38. Klementiev, K., XAFSmass, freeware: www. cells. es/Beamlines. *CLAESS/software/xafsmass. html*.
39. Wu, Y.; Fan, L.; Chen, S.; Chen, S.; Zou, C.; Wu, Z., Spectroscopic analysis of phase constitution of high quality VO2 thin film prepared by facile sol-gel method. *AIP Advances* **2013,** 3, (4), 042132.
40. Li, S. Y.; Niklasson, G. A.; Granqvist, C. G., Thermochromism of VO2 nanoparticles: Calculated optical properties and applications to energy efficient windows. *MRS Online Proc. Libr.* **2011,** 1315, (Copyright (C) 2013 American Chemical Society (ACS). All Rights Reserved.).